Yoash Levron
The Andrew and Erna Viterbi Faculty of Electrical Engineering, Technion—Israel Institute of Technology, Haifa 3200003, Israel
yoashl@ee.technion.ac.il

Juri Belikov
Department of Software Science, Tallinn University of Technology, Akadeemia tee 15a, 12618 Tallinn, Estonia
juri.belikov@taltech.ee

Lecture 1: Introduction to Power System Dynamics: Time-varying Phasors and Primary Frequency Control

Abstract

This lecture is a short introduction to power system dynamics. It discusses the approximation of time-varying phasors, and reviews key aspects of the primary and secondary control mechanisms.

Introduction

Time-varying phasor models are used extensively in power system analysis [1–4]. In such models it is assumed that voltages and currents are nearly sinusoidal, and therefore can be described by means of phasors, which amplitude and phase vary slowly over time. One advantage of time-varying phasor models is that they use "natural" signals of amplitudes, phases, and powers, which are intuitive to power engineers. An additional advantage is that such models do not include sinusoidal components, and therefore have well-defined equilibrium points. Due to these properties time-varying phasors are frequently used for stability analysis and for modeling relatively slow transients [4–18].

Despite these advantages, it is important to keep in mind that time-varying phasors are an approximation, and can only be used if variations in amplitudes and phases are indeed slow. Therefore, one objective of this lecture is to highlight the assumptions which enable modeling based on time-varying phasors. This lecture also serves as an introduction to more advanced modeling techniques, such as in [19–25], which will be discussed in the following lectures.

Time-varying phasors

When describing complex dynamic systems it is imperative to choose the model according to the time scale of interest. Transient models, which use physical signals such as instantaneous voltages and currents, are a natural choice for describing fast phenomena such as faults, lightning strikes, etc. However, one disadvantage of transient models is their complexity. Specifically, since voltage and current signals are sinusoidal at steady-state, the system does not have an equilibrium point (in the usual sense), and cannot be studied based on small-signal approximations. Therefore, while detailed transient models allow accurate simulations, they are generally not suitable for analytic stability studies [19, 26, 27].

A common approach to simplify the analysis of complex dynamic phenomena in AC power systems is to use the approximation of time-varying phasors. In such models it is assumed that voltages and currents are nearly sinusoidal, and therefore can be described by means of phasors, which amplitude and phase vary slowly over time. Consider an AC signal, which amplitude and phase are time dependent,

$$v(t) = \sqrt{2}|V(t)|\cos(\omega_r t + \angle V(t)), \tag{1}$$

Series of lectures on power system dynamics. The lectures are freely available on https://a-lab.ee/projects/dq0-dynamics

where ω_r is the *reference frequency*, and $\omega_r t$ is the *reference phase*. While the amplitude $|V(t)|$ and phase $\angle V(t)$ vary with time, a key assumption is that these signals are nearly constant over a 50Hz/60Hz cycle. Therefore, if changes in the amplitude and phase are slow, then at a small time-interval around t the signal can be represented by a phasor

$$V(t) = |V(t)|\angle V(t). \tag{2}$$

This idea is illustrated in Fig. 1.

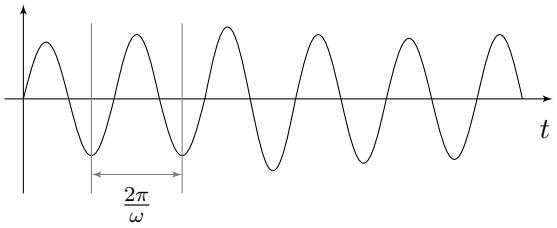

Figure 1: Signals that are nearly sinusoidal are described as time-varying phasors. The amplitude and phase vary with time, but are nearly constant over a single 50Hz/60Hz cycle.

Time-varying phasors use "natural" signals of amplitudes, phases, and powers, which are intuitive to power engineers. In addition, time-varying phasors map AC signals to constants. The resulting dynamic model has well-defined equilibrium points, and therefore it can be linearized and studied based on standard linear systems theory. Table 1 compares the advantages and disadvantages of transient models and time-varying phasor models.

Table 1: Comparison of transient models and time-varying phasor models

	equilibrium points	small-signal	fast transients
transient models	X	X	✓
time-varying phasors	✓	✓	X

Consider a general balanced three-phase unit, as shown in Fig. 2.

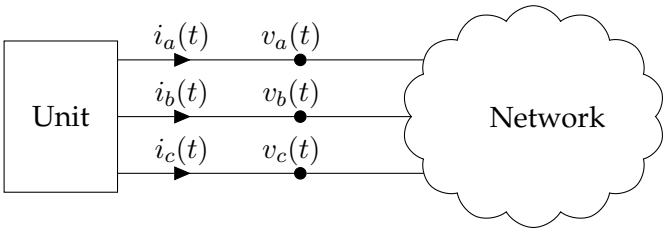

Figure 2: A general three-phase unit.

Assume that the grid is balanced, and that voltages and currents are described by time-varying phasors $V(t)$, $I(t)$. The reference angle of the system is defined as θ_r. For a constant reference frequency this angle is given by $\theta_r = \omega_r t$, and in general

$$\frac{\mathrm{d}}{\mathrm{d}t}\theta_r = \omega_r, \tag{3}$$

where ω_r is the reference frequency. The corresponding signals in the time domain are

$$\begin{aligned}
v_a(t) &= \sqrt{2}|V(t)|\cos(\theta_r(t)+\angle V(t)),\\
v_b(t) &= \sqrt{2}|V(t)|\cos\left(\theta_r(t)+\angle V(t)-\frac{2\pi}{3}\right),\\
v_c(t) &= \sqrt{2}|V(t)|\cos\left(\theta_r(t)+\angle V(t)+\frac{2\pi}{3}\right),\\
i_a(t) &= \sqrt{2}|I(t)|\cos(\theta_r(t)+\angle I(t)),\\
i_b(t) &= \sqrt{2}|I(t)|\cos\left(\theta_r(t)+\angle I(t)-\frac{2\pi}{3}\right),\\
i_c(t) &= \sqrt{2}|I(t)|\cos\left(\theta_r(t)+\angle I(t)+\frac{2\pi}{3}\right).
\end{aligned} \tag{4}$$

In addition, the active and reactive powers flowing from the unit into the network are

$$\begin{aligned}
P(t) &= \mathrm{Re}\{V(t)I^*(t)\},\\
Q(t) &= \mathrm{Im}\{V(t)I^*(t)\}.
\end{aligned} \tag{5}$$

Recall that in a balanced three-phase system the active power has two different meanings:

- ✓ $P(t)$ is the *average* power over a cycle, for a single phase.
- ✓ $3P(t)$ is the three-phase *instantaneous* power. This power is **approximately constant** throughout a single cycle since for a balanced three-phase system

$$v_a(t)i_a(t)+v_b(t)i_b(t)+v_c(t)i_c(t) \approx 3\,\mathrm{Re}\{V(t)I^*(t)\} = 3P(t). \tag{6}$$

A general approach for constructing signal flow diagrams based on time-varying phasors is described next. First the system is divided into the transmission network and the units connected to it. The interface between each unit and the network includes four signals:

- ✓ $P_i(t)$ is the (single-phase) active power flowing from the unit into the network.
- ✓ $Q_i(t)$ is the reactive power flowing from the unit into the network.
- ✓ $|V_i(t)|$ is the voltage amplitude.
- ✓ $\angle V_i(t) = \delta_i$ is the voltage phase.

This idea is illustrated in Fig. 3.

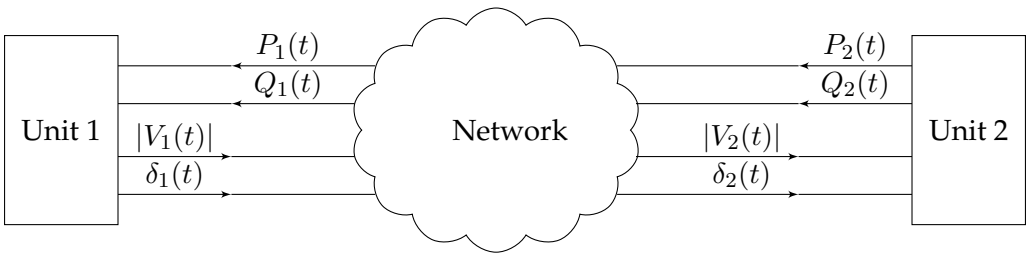

Figure 3: A general signal-flow diagram based on time-varying phasors.

Under the assumption of time-varying phasors, the transmission network is described by a set of algebraic equations

$$I(t) = YV(t) \quad \text{or} \quad V(t) = ZI(t), \tag{7}$$

where Y is the admittance matrix, and Z is the impedance matrix. Note that currents are considered positive when flowing into the network. We often denote $Y = Y(j\omega_s)$ and $Z = Z(j\omega_s)$ to indicate that these matrices are constant and evaluated at $s = j\omega_s$, where ω_s is the nominal system frequency. In a simple network, in which every two buses are connected by a single admittance, the matrix Y is constructed as follows:

- ✓ $y_{i,i}$ is the sum of admittances connected to bus i,
- ✓ $y_{i,n}$ is minus the admittance connecting buses i and n.

Equivalently, the network is often described by the *power flow* equations, which are developed next. Using (7),

$$\begin{aligned} I_i(t) &= \sum_{n=1}^{N} y_{i,n} V_n(t), \\ V_i^*(t) I_i(t) &= \sum_{n=1}^{N} y_{i,n} V_n(t) V_i^*(t), \end{aligned} \tag{8}$$

and since $V_i(t) I_i^*(t) = P_i(t) + jQ_i(t)$,

$$P_i(t) - jQ_i(t) = \sum_{n=1}^{N} y_{i,n} V_n(t) V_i^*(t). \tag{9}$$

Now, using the notation $\delta_i(t) = \angle V_i(t)$ we have

$$P_i(t) - jQ_i(t) = \sum_{n=1}^{N} |y_{i,n}||V_n(t)||V_i(t)| \exp\left(j\delta_n(t) - j\delta_i(t) + j\angle y_{i,n}\right), \tag{10}$$

and the real and imaginary parts of this equation are

$$\begin{aligned} P_i(t) &= \sum_{n=1}^{N} |y_{i,n}||V_n(t)||V_i(t)| \cos\left(\delta_n(t) - \delta_i(t) + \angle y_{i,n}\right), \\ Q_i(t) &= -\sum_{n=1}^{N} |y_{i,n}||V_n(t)||V_i(t)| \sin\left(\delta_n(t) - \delta_i(t) + \angle y_{i,n}\right). \end{aligned} \tag{11}$$

These are known as the *power flow* equations. Sometimes these nonlinear equations are simplified using the *DC power flow* approximation, which is described next. Assume that

- ✓ Transmission lines are nearly inductive with impedances $jX_{i,n}$.
- ✓ The voltage amplitudes are nearly constant, $|V_i(t)| \approx |V|$.
- ✓ The voltage phases are nearly equal, $\delta_i(t) \approx \delta_n(t)$.

Based on these assumptions the power flow equations in (11) may be approximated as

$$\begin{aligned} P_i(t) &\approx \sum_{n \neq i} \frac{|V|^2}{X_{i,n}} \left(\delta_i - \delta_n\right), \\ Q_i(t) &\approx 0. \end{aligned} \tag{12}$$

Note that the active power is a linear function of the voltage phases.

The synchronous generator

This section presents a dynamic model of the synchronous generator. For the sake of clarity, the model shown here is based on the approximation of time-varying phasors, and is therefore only valid for slow transients. In addition, the complex dynamic equations of the prime-mover are considerably simplified. These approximations will be revised in the following lectures. A basic diagram of the synchronous machine is shown in Fig. 4. A single-phase electric diagram of a balanced machine is shown in Fig. 5.

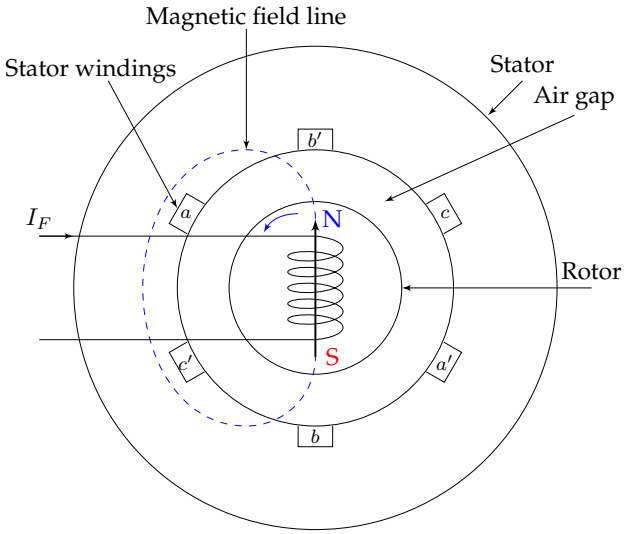

Figure 4: Simplified structure of the synchronous machine.

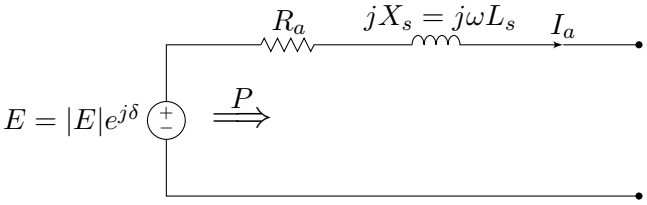

Figure 5: Simplified single-phase diagram of a balanced synchronous machine.

Often the resistance and inductance in Fig. 5 are analyzed as part of the transmission network, so the machine is represented only by the internal voltage source on the left. In Fig 5:

- ✓ $|E|$ is the magnitude of the internal voltage source.
- ✓ δ is the phase of the internal voltage source. This angle is often called the *power angle*.
- ✓ R_a is the stator winding resistance.
- ✓ L_s is the synchronous inductance.
- ✓ I_a is the current in the stator windings (this is a phasor).
- ✓ P is the active power provided by the internal voltage source (for a single phase).

We will now develop a dynamic model of the generator with inputs and outputs as shown in Fig. 6.

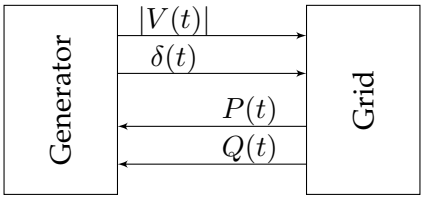

Figure 6: Inputs and outputs of the synchronous generator model.

Define the following quantities:

- ✓ P_m is the mechanical power accelerating the rotor.
- ✓ J is the rotor moment of inertia.
- ✓ p_f is the number of magnetic poles on the rotor (must be even).
- ✓ θ is the rotor electrical angle.
- ✓ $\omega = \frac{\mathrm{d}}{\mathrm{d}t}\theta$ is the rotor electrical frequency.
- ✓ $\theta_m = (2/p_f)\theta$ is the rotor's mechanical angle, relative to a fixed point on the stator.
- ✓ $\omega_m = \frac{\mathrm{d}}{\mathrm{d}t}\theta_m$ is the rotor mechanical frequency.
- ✓ ω_s is the nominal system frequency ($\omega_s = 2\pi 50$ or $2\pi 60$ rad/s).
- ✓ D is the damping coefficient.
- ✓ P_{ref} is the reference power.
- ✓ $K = \left(\frac{p_f}{2}\right)^2 \frac{1}{J\omega_s} =$ constant.

The basic relations between angles and frequencies are

$$\begin{aligned} \omega &= \frac{\mathrm{d}}{\mathrm{d}t}\theta, \\ \theta_m &= \frac{2}{p_f}\theta, \\ \omega_m &= \frac{\mathrm{d}}{\mathrm{d}t}\theta_m = \frac{2}{p_f}\omega. \end{aligned} \tag{13}$$

In addition, the angular acceleration is proportional to the total torque acting on the rotor

$$\frac{\mathrm{d}}{\mathrm{d}t}\omega_m = \frac{1}{J}(T_m - T_e), \tag{14}$$

or equivalently

$$\frac{\mathrm{d}}{\mathrm{d}t}\omega = \frac{p_f}{2J}(T_m - T_e), \tag{15}$$

where T_m is the mechanical torque accelerating the rotor, and T_e is the electrical torque that decelerates it. In addition, torques and powers are related by

$$\begin{aligned} P_m = T_m\omega_m &= \frac{2}{p_f}T_m\omega, \\ 3P = T_e\omega_m &= \frac{2}{p_f}T_e\omega. \end{aligned} \tag{16}$$

Substitution yields

$$\frac{\mathrm{d}}{\mathrm{d}t}\omega = \left(\frac{p_f}{2}\right)^2 \frac{1}{J\omega}(P_m - 3P), \tag{17}$$

and the approximation $\omega \approx \omega_s$ leads to

$$\frac{\mathrm{d}}{\mathrm{d}t}\omega = \left(\frac{p_f}{2}\right)^2 \frac{1}{J\omega_s}(P_m - 3P). \tag{18}$$

Here ω_s is the nominal system frequency, $\omega_s = 2\pi 50$ or $2\pi 60$ rad/s. Now, using the constant $K = \left(\frac{p_f}{2}\right)^2 \frac{1}{J\omega_s}$ defined above we obtain

$$\frac{\mathrm{d}}{\mathrm{d}t}\omega = K(P_m - 3P). \tag{19}$$

This equation describes the rotor dynamics, and is known as the *swing equation*. The rotor accelerates if the mechanical power is larger than the electrical power $P_m > 3P$, and decelerates if $P_m < 3P$. In case $P_m = 3P$ the frequency is constant, and the generator operates at steady-state. In addition, the mechanical power is typically controlled as follows:

$$P_m = 3P_{ref} - \frac{1}{D}(\omega - \omega_s). \tag{20}$$

This equation describes the *frequency droop* controller. As we shall see in the following sections this type of control is crucial for regulating the frequency and maintaining stability. Note that this linear relationship ignores the complex dynamics of the prime-mover, and holds only for slow transients. Substituting this last expression in (19) yields

$$\frac{\mathrm{d}}{\mathrm{d}t}\omega = K\left(3P_{ref} - 3P - \frac{1}{D}(\omega - \omega_s)\right), \tag{21}$$

which is another form of the swing equation.

The dynamics of the power angle (δ) is described next. This angle is defined as [28]

$$\begin{aligned} \delta &= \theta - \theta_r + \frac{\pi}{2}, \\ \frac{\mathrm{d}}{\mathrm{d}t}\delta &= \omega - \omega_r, \end{aligned} \tag{22}$$

where θ_r is the reference angle and $\omega_r = \mathrm{d}\theta_r/\mathrm{d}t$ is the reference frequency, as discussed above. For now we will assume that the reference frequency is constant, and is equal to the nominal frequency:

$$\theta_r = \omega_s t \quad \Rightarrow \quad \omega_r = \omega_s. \tag{23}$$

This assumption will be revised in the following sections. This selection of the reference angle yields

$$\frac{\mathrm{d}}{\mathrm{d}t}\delta = \omega - \omega_s, \tag{24}$$

and the resulting dynamic model of the generator is

$$\begin{aligned} \frac{\mathrm{d}}{\mathrm{d}t}\delta &= \omega - \omega_s = \Delta\omega, \\ \frac{\mathrm{d}}{\mathrm{d}t}\Delta\omega &= K\left(3P_{ref} - 3P - \frac{1}{D}\Delta\omega\right). \end{aligned} \tag{25}$$

This model is described by the block diagram in Fig. 7. In this model:

✓ The state variables are δ and $\Delta\omega = \omega - \omega_s$. These are the outputs of the two integrators.

✓ The inputs of the model are P and P_{ref}.

✓ The outputs of the model are $|V|$ and δ.

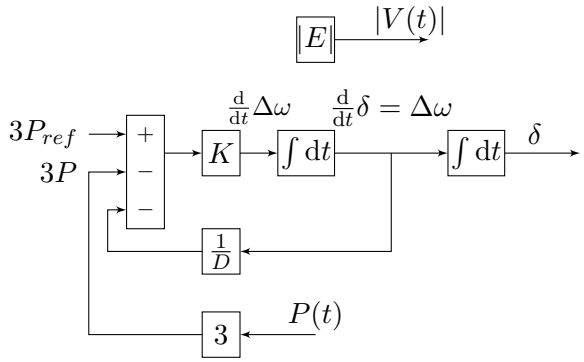

Figure 7: Dynamic model of the synchronous generator with a reference frequency $\omega_r = \omega_s$.

Example: synchronous generator connected to an infinite bus

Consider the single-phase diagram in Fig. 8, which describes a synchronous generator connected to an infinite bus. The grid is represented by an ideal voltage source with a constant amplitude V_g, zero phase, and a constant frequency ω_s. The system is described by the signal flow diagram in Fig. 9.

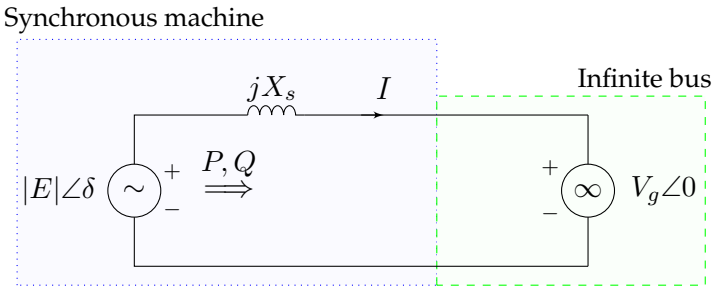

Figure 8: Generator connected to an infinite bus, single-phase diagram.

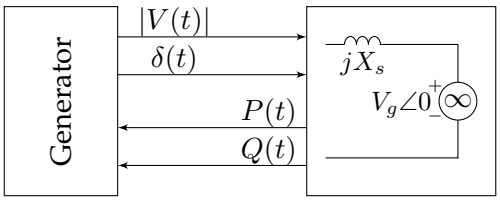

Figure 9: Generator connected to an infinite bus: signal flow diagram.

The generator is modeled as shown in Fig. 7, and the electric network is described as

$$\begin{aligned} I &= \frac{1}{jX_s}\left(|E|e^{j\delta} - V_g\right), \\ P &= \mathrm{Re}\left\{|E|e^{j\delta}I^*\right\}, \end{aligned} \tag{26}$$

which lead to

$$\begin{aligned} P &= \mathrm{Re}\left\{ |E|e^{j\delta}\left(|E|e^{-j\delta} - V_g\right)\frac{1}{-jX_s}\right\} = \mathrm{Re}\left\{\frac{j}{X_s}\left(|E|^2 - |E|V_g e^{j\delta}\right)\right\} \\ &= \mathrm{Re}\left\{\frac{j}{X_s}\left(|E|^2 - |E|V_g\cos(\delta) - j|E|V_g\sin(\delta)\right)\right\} = \frac{|E|V_g}{X_s}\sin(\delta). \end{aligned} \tag{27}$$

A block diagram of the system is shown in Fig. 10.

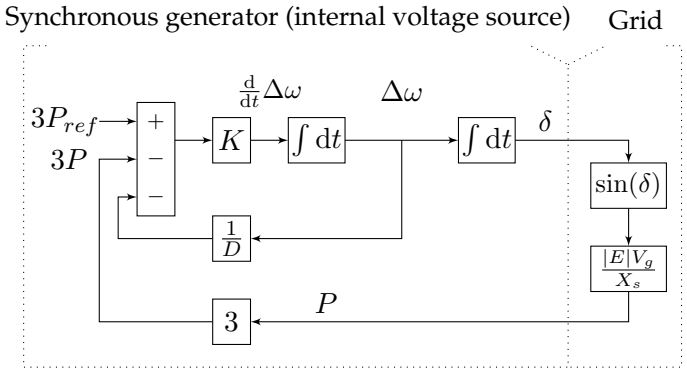

Figure 10: Generator connected to an infinite bus: block diagram.

The system can now be analyzed as follows:

- ✓ Calculate the equilibrium points,
- ✓ Linearize the system in the neighborhood of each equilibrium point,
- ✓ Compute the transfer function of the linear system, and test its stability.

To this end, the state variables, inputs and outputs are expressed as

$$\begin{aligned} x &= \bar{x} + \hat{x}, \\ u &= \bar{u} + \hat{u}, \\ y &= \bar{y} + \hat{y}, \end{aligned} \tag{28}$$

where x, y, u are the original signals, $\bar{x}$, $\bar{u}$, $\bar{y}$ denote the equilibrium point, and $\hat{x}$, $\hat{u}$, $\hat{y}$ are "small" signals.

Equilibrium points

The equilibrium points may be calculated by zeroing the time derivatives. In this example:

$$\begin{aligned} \frac{\mathrm{d}}{\mathrm{d}t}\delta &= 0, \\ \frac{\mathrm{d}}{\mathrm{d}t}\Delta\omega &= 0. \end{aligned} \tag{29}$$

Equivalently, the inputs of the integrators must be zero. Based on Fig. 10,

$$\Delta\bar{\omega} = \bar{\omega} - \omega_s = 0, \quad \bar{P} = \bar{P}_{ref}. \tag{30}$$

It follows that the frequency $\bar{\omega}$ and the generator's active power $\bar{P}$ are specified at an equilibrium point. As a result, in a power flow analysis the generator can be described as a P-V bus, with given active power and voltage magnitude:

$$\begin{aligned} |\bar{V}| &= |E| \quad \text{(known)}, \\ \bar{P} &= \bar{P}_{ref} \quad \text{(known)}. \end{aligned} \tag{31}$$

In other words, the equilibrium points may be found by solving the power flow equations of the system shown in Fig. 11.

Figure 11: Generator connected to an infinite bus: single-line diagram.

In this example the power flow equations may be solved analytically, and based on (27) the solution is

$$\bar{P} = \frac{|E|V_g}{X_s}\sin(\bar{\delta}) = P_{ref}, \tag{32}$$

which yields two possible equilibrium points:

$$\begin{aligned} \bar{\delta}_1 &= \sin^{-1}\left(\frac{X_s\bar{P}_{ref}}{|E|V_g}\right), \\ \bar{\delta}_2 &= \pi - \sin^{-1}\left(\frac{X_s\bar{P}_{ref}}{|E|V_g}\right). \end{aligned} \tag{33}$$

As a general rule, when the system is connected to an infinite bus, the equilibrium points can always be found by solving the power flow equations.

Linearization

The block diagram in Fig. 10 includes linear components, and one nonlinear component $\sin(\delta)$ which is a memoryless function. Recall that such a block diagram can be directly linearized as follows:

- ✓ The original signals are replaced by "small" signals.
- ✓ Linear components remain unchanged.
- ✓ Constants are zeroed.
- ✓ Nonlinear functions are replaced by constant gains, which are the nonlinear functions' derivatives at the equilibrium point.

Applying this process to the system in Fig. 10 leads to the linear system shown in Fig. 12.

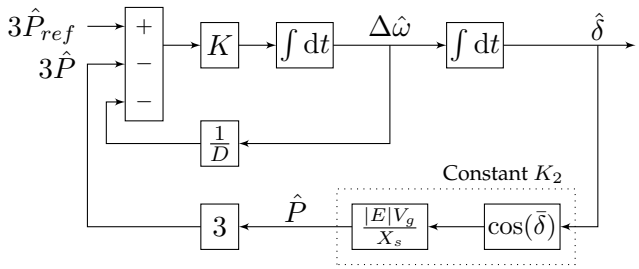

Figure 12: Generator connected to an infinite bus: linearized model.

The equivalent state space model is

$$\begin{aligned}\frac{\mathrm{d}}{\mathrm{d}t}\begin{bmatrix}\hat{\delta}\\ \Delta\hat{\omega}\end{bmatrix} &= \begin{bmatrix}0 & 1\\ -3KK_2 & -\frac{K}{D}\end{bmatrix}\begin{bmatrix}\hat{\delta}\\ \Delta\hat{\omega}\end{bmatrix} + \begin{bmatrix}0\\ 3K\end{bmatrix}\hat{P}_{ref},\\ \begin{bmatrix}\hat{\delta}\\ \hat{P}\end{bmatrix} &= \begin{bmatrix}1 & 0\\ K_2 & 0\end{bmatrix}\begin{bmatrix}\hat{\delta}\\ \Delta\hat{\omega}\end{bmatrix},\end{aligned} \tag{34}$$

and the constants are

$$K = \left(\frac{p_f}{2}\right)^2 \frac{1}{J\omega_s}, \quad K_2 = \frac{|E|V_g}{X_s}\cos(\bar{\delta}). \tag{35}$$

The outputs are chosen arbitrarily, and can be replaced by other signals of interest.

Transfer functions and stability

The transfer function of the system is given by

$$H(s) = \begin{bmatrix}\frac{\hat{\delta}(s)}{\hat{P}_{ref}(s)}\\ \frac{\hat{P}(s)}{\hat{P}_{ref}(s)}\end{bmatrix} = C(sI - A)^{-1}B, \tag{36}$$

where A, B, C are the matrices in (34). Using Cramer's rule for matrix inversion we have

$$H(s) = \frac{\begin{bmatrix}1 & 0\\ K_2 & 0\end{bmatrix}\begin{bmatrix}s + K/D & 1\\ -3KK_2 & s\end{bmatrix}\begin{bmatrix}0\\ 3K\end{bmatrix}}{s(s + K/D + 3KK_2)}, \tag{37}$$

which leads to

$$\begin{aligned}\frac{\hat{\delta}(s)}{\hat{P}_{ref}(s)} &= \frac{3K}{s^2 + \frac{K}{D}s + 3KK_2},\\ \frac{\hat{P}(s)}{\hat{P}_{ref}(s)} &= \frac{3KK_2}{s^2 + \frac{K}{D}s + 3KK_2}.\end{aligned} \tag{38}$$

The poles of the system are the roots of the characteristic polynomial:

$$\det(sI - A) = s^2 + \frac{K}{D}s + 3KK_2 = 0, \tag{39}$$

$$s_{1,2} = -\frac{K}{2D} \pm \frac{1}{2}\sqrt{\left(\frac{K}{D}\right)^2 - 12KK_2}. \tag{40}$$

Recall that an equilibrium point is stable if the poles are on the left side of the complex plane, that is $\mathrm{Re}(s) < 0$. In this example the possible cases are

- ✓ $K_2 > 0$ and $\left(\frac{K}{D}\right)^2 - 12KK_2 < 0$: the roots are complex, and $\mathrm{Re}\{s_{1,2}\} = -\frac{K}{2D} < 0$.
- ✓ $K_2 > 0$ and $\left(\frac{K}{D}\right)^2 - 12KK_2 \geq 0$: the roots are real, and $s_1 < 0$, $s_2 < 0$.
- ✓ $K_2 < 0$: the roots are real, and $s_1 > 0$, $s_2 < 0$.
- ✓ $K_2 = 0$: the roots are real, and $s_1 = 0$, $s_2 < 0$.

To summarize,

- ✓ If $K_2 > 0$ the poles have real negative parts. In this case the equilibrium point is *stable*.

- ✓ If $K_2 < 0$ there exists a pole with real positive part. In this case the equilibrium point is *unstable*.
- ✓ If $K_2 = 0$ there is a pole on the imaginary axis. In this case the linear model does not provide sufficient information to determine stability.

Based on (33), the equilibrium points are

$$\begin{aligned} \bar{\delta}_1 &= \sin^{-1}\left(\frac{X_s P_{ref}}{|E|V_g}\right) \leq \frac{\pi}{2}, \\ \bar{\delta}_2 &= \pi - \sin^{-1}\left(\frac{X_s P_{ref}}{|E|V_g}\right) \geq \frac{\pi}{2}, \end{aligned} \tag{41}$$

and therefore

$$\begin{aligned} \text{for} \quad \bar{\delta}_1 : \quad K_2 &= \frac{|E|V_g}{X_s}\cos(\bar{\delta}_1) \geq 0, \\ \text{for} \quad \bar{\delta}_2 : \quad K_2 &= \frac{|E|V_g}{X_s}\cos(\bar{\delta}_2) \leq 0. \end{aligned} \tag{42}$$

Assuming that $K_2 \neq 0$, $\bar{\delta}_1$ is a **stable** equilibrium point, and $\bar{\delta}_2$ is an **unstable** equilibrium point. Recall that these two points correspond to two solutions of the power flow equations. The analysis above shows that only the solution with $\bar{\delta} \leq \frac{\pi}{2}$ is stable. The other solution with $\bar{\delta} \geq \frac{\pi}{2}$ is unstable, and therefore cannot occur in a realistic system.

More generally each solution of the power flow equations describes a possible equilibrium point. However, the system can only work in the neighborhood of stable equilibrium points, so unstable points do not represent physical solutions.

Multiple generators, connected to an infinite bus

This section presents a dynamic model of several machines which are connected to an infinite bus. It is assumed that

- ✓ Bus 1 is an infinite bus, with a frequency ω_s.
- ✓ The resistances and synchronous inductances of the generators are included in the transmission network model.

The first step is to calculate the equilibrium points, by solving the power flow equations. Next, the dynamic model can be constructed based on the generator block diagram in Fig. 7. A general block diagram of the system is presented in Fig. 13.

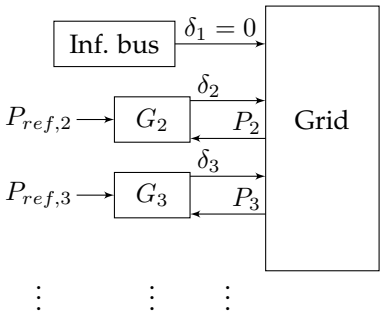

Figure 13: Multiple generators connected to an infinite bus: block diagram.

As an example, consider the system in Fig. 14.

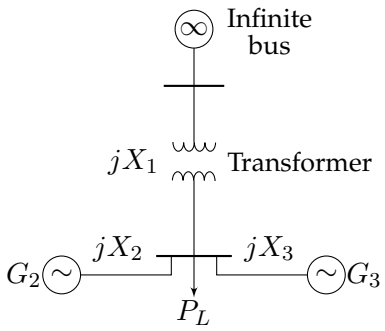

Figure 14: Example: two generators connected to an infinite bus. jX_1 is the transformer's leakage impedance in per-unit (pu), and jX_2, jX_3 are the synchronous impedances of the generators in per-unit.

The transmission network is modeled based on the DC power flow approximation. For this purpose it is assumed that the voltages in all buses are equal to 1 pu. The resulting equations are

$$\begin{aligned} \delta_1 &= 0 \\ P_1 &= \frac{1}{X_1}(\delta_1 - \delta_4), \\ P_2 &= \frac{1}{X_2}(\delta_2 - \delta_4), \\ P_3 &= \frac{1}{X_3}(\delta_3 - \delta_4), \\ P_1 + P_2 + P_3 &= P_L, \quad (P_L \text{ is positive}). \end{aligned} \tag{43}$$

By substitution we obtain

$$\delta_4 = \frac{\frac{\delta_2}{X_2} + \frac{\delta_3}{X_3} - P_L}{\frac{1}{X_1} + \frac{1}{X_2} + \frac{1}{X_3}}, \tag{44}$$

which leads to

$$\begin{aligned} P_2 &= \frac{(X_1 + X_3)\delta_2 - X_1\delta_3 + X_1X_3P_L}{X_1X_3 + X_2(X_1 + X_3)}, \\ P_3 &= \frac{(X_1 + X_2)\delta_3 - X_1\delta_2 + X_1X_2P_L}{X_1X_2 + X_3(X_1 + X_2)}. \end{aligned} \tag{45}$$

These relations may be expressed as

$$\begin{bmatrix} P_2 \\ P_3 \end{bmatrix} = U_{2\times 2} \begin{bmatrix} \delta_2 \\ \delta_3 \end{bmatrix} + W_{2\times 1} P_L, \tag{46}$$

where $U_{2\times 2}$ and $W_{2\times 1}$ are constant matrices. Using this result, the equilibrium point is the solution of

$$\begin{bmatrix} \bar{P}_2 \\ \bar{P}_3 \end{bmatrix} = U \begin{bmatrix} \bar{\delta}_2 \\ \bar{\delta}_3 \end{bmatrix} + W\bar{P}_L = \begin{bmatrix} \bar{P}_{ref,2} \\ \bar{P}_{ref,3} \end{bmatrix}, \tag{47}$$

and if U is invertible then

$$\begin{bmatrix} \bar{\delta}_2 \\ \bar{\delta}_3 \end{bmatrix} = U^{-1} \left(\begin{bmatrix} \bar{P}_{ref,2} \\ \bar{P}_{ref,3} \end{bmatrix} - W\bar{P}_L \right). \tag{48}$$

A block diagram of the system is shown in Fig. 15.

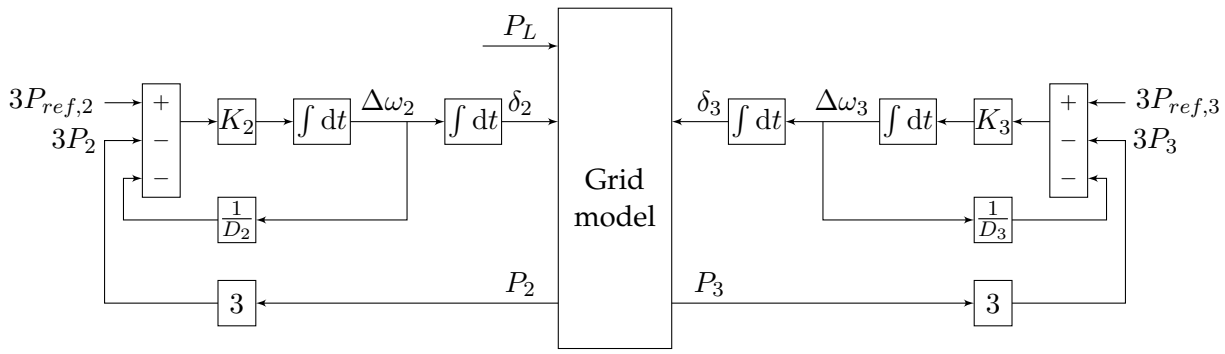

Figure 15: Two generators connected to an infinite bus: block diagram.

Note that this model is linear since we used the DC power flow approximation. As usual, the outputs of the integrators are chosen as state variables, and the resulting model is

$$\begin{aligned}\frac{\mathrm{d}}{\mathrm{d}t}\begin{bmatrix}\delta_2\\ \delta_3\\ \Delta\omega_2\\ \Delta\omega_3\end{bmatrix} &= \begin{bmatrix} 0 & 0 & 1 & 0 \\ 0 & 0 & 0 & 1 \\ -3\begin{bmatrix} K_2 & 0 \\ 0 & K_3 \end{bmatrix} U_{2\times 2} & & \begin{matrix} -\frac{K_2}{D_2} & 0 \\ 0 & -\frac{K_3}{D_3} \end{matrix} \end{bmatrix}\begin{bmatrix}\delta_2\\ \delta_3\\ \Delta\omega_2\\ \Delta\omega_3\end{bmatrix} \\ &+ \begin{bmatrix} 0 & 0 & 0 \\ 0 & 0 & 0 \\ 3K_2 & 0 & -3\begin{bmatrix} K_2 & 0 \\ 0 & K_3 \end{bmatrix} W_{2\times 1} \\ 0 & 3K_3 & \end{bmatrix}\begin{bmatrix}P_{ref,2}\\ P_{ref,3}\\ P_L\end{bmatrix},\end{aligned} \tag{49}$$

$$y = \begin{bmatrix}\delta_2\\ \delta_3\\ P_2\\ P_3\end{bmatrix} = \begin{bmatrix} 1 & 0 & 0 & 0 \\ 0 & 1 & 0 & 0 \\ & & 0 & 0 \\ U_{2\times 2} & & 0 & 0 \end{bmatrix}\begin{bmatrix}\delta_2\\ \delta_3\\ \Delta\omega_2\\ \Delta\omega_3\end{bmatrix} + \begin{bmatrix} 0 \\ 0 \\ W_{2\times 1} \end{bmatrix} P_L. \tag{50}$$

The outputs are chosen arbitrarily, and can be replaced by other signals of interest.

Multiple generators, without connection to an infinite bus

In the previous sections it was assumed that one of the buses is an infinite bus, with a constant frequency ω_s. Recall that the reference angle was defined in this case as $\theta_r = \omega_s t$, and the power angles δ_i were defined accordingly:

$$\begin{aligned}\delta_i &= \theta_i - \theta_r + \frac{\pi}{2} = \theta_i - \omega_s t + \frac{\pi}{2}, \\ \frac{\mathrm{d}}{\mathrm{d}t}\delta_i &= \omega_i - \omega_s = \Delta\omega_i.\end{aligned} \tag{51}$$

If the system is not connected to an infinite bus this definition is no longer useful, since there is no generator that rotates at a frequency of ω_s. In this case the reference angle should be chosen differently, and is usually defined with respect to the electric angle of the first generator:

$$\theta_r = \theta_1 + \frac{\pi}{2}. \tag{52}$$

Other choices of the reference angle are possible, but will not be used in this text. In this reference frame the power angles are defined as

$$\begin{aligned}\delta_i &= \theta_i - \underbrace{\left(\theta_1 + \frac{\pi}{2}\right)}_{\theta_r} + \frac{\pi}{2} = \theta_i - \theta_1, \\ \frac{\mathrm{d}}{\mathrm{d}t}\delta_i &= \omega_i - \omega_1.\end{aligned} \tag{53}$$

This new reference frame is the only change needed to construct a dynamic model. The amplitude of the internal voltage remains unchanged:

$$E_i = |E_i|\angle\delta_i, \tag{54}$$

and generator 1 serves as a reference:

$$\delta_1 = \theta_1 - \theta_1 = 0. \tag{55}$$

In addition, the swing equation remains unchanged:

$$\frac{\mathrm{d}}{\mathrm{d}t}\omega_i = K_i\left(3P_{ref,i} - 3P_i - \frac{1}{D_i}\left(\omega_i - \omega_s\right)\right), \tag{56}$$

where ω_s is the nominal frequency ($2\pi 50$ or $2\pi 60$ rad/s). This frequency is now used only as part of the control mechanism, and does not represent the frequency of a specific generator. Based on these results , the dynamic model of the generator is

$$\begin{aligned}\frac{\mathrm{d}}{\mathrm{d}t}\delta_i &= \omega_i - \omega_1, \\ \frac{\mathrm{d}}{\mathrm{d}t}\omega_i &= K_i\left(3P_{ref,i} - 3P_i - \frac{1}{D_i}\left(\omega_i - \omega_s\right)\right).\end{aligned} \tag{57}$$

A block diagram describing this model is shown in Fig. 16. A block diagram of generator 1 is shown separately in Fig. 17.

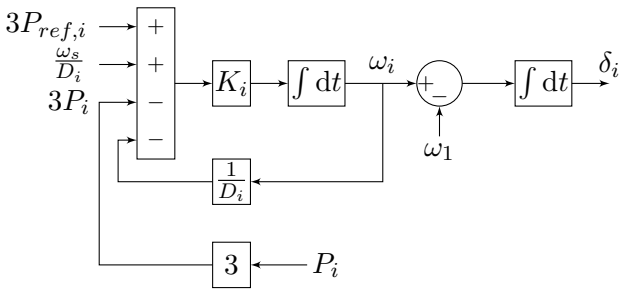

Figure 16: Dynamic model of a synchronous generator with a reference angle $\theta_r = \theta_1 + \frac{\pi}{2}$.

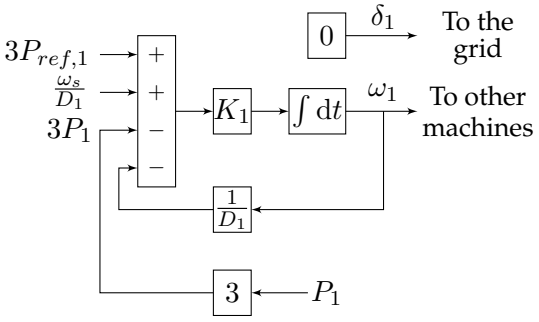

Figure 17: Dynamic model of generator 1, with a reference frequency $\theta_r = \theta_1 + \frac{\pi}{2}$.

As an example, consider a power system with two generators and a load, as shown in Fig. 18. Note that there is no connection to an infinite bus. The block diagram of the system is presented in Fig. 19.

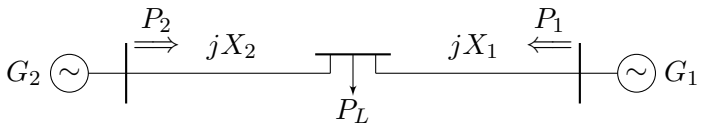

Figure 18: Example: two generators feeding a load.

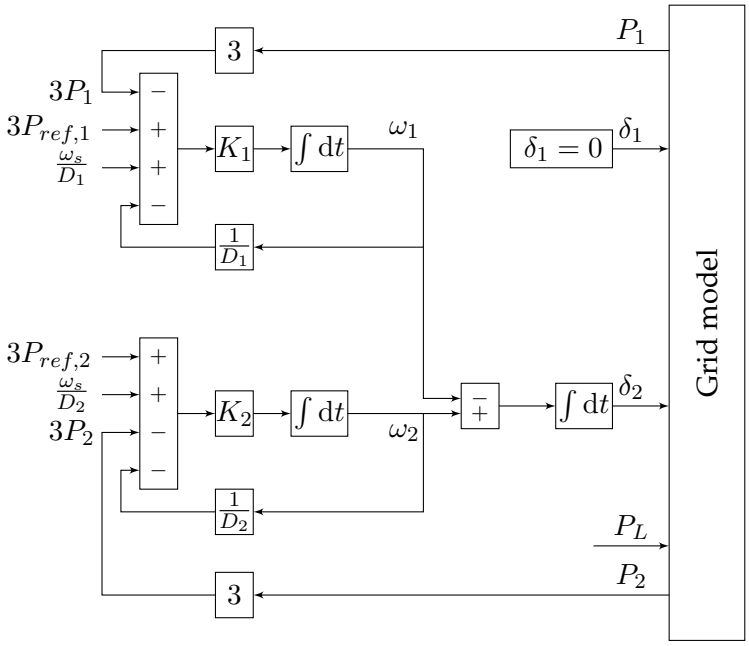

Figure 19: Two generators feeding a load: block diagram.

The transmission network is described based on the DC power flow equations:

$$\begin{aligned} P_1 &= -\frac{\delta_2}{X_1+X_2} + \frac{X_2}{X_1+X_2}P_L, \\ P_2 &= \frac{\delta_2}{X_1+X_2} + \frac{X_1}{X_1+X_2}P_L. \end{aligned} \tag{58}$$

Frequency droop control

In the previous sections we have assumed a linear relationship between the mechanical power and frequency:

$$P_{m,i} = 3P_{ref,i} - \frac{1}{D_i}\left(\omega_i - \omega_s\right). \tag{59}$$

This control law is often named *primary frequency control*, *frequency droop control*, or simply *droop control*[1]. As we shall see in this section, the objectives of this control law are

- ✓ To regulate the frequency and active power.
- ✓ To promote fair sharing of active power among generators.
- ✓ To allow generators of different sizes to operate in parallel.

[1]Recall that this relation ignores the complex dynamics of the mechanical system, and holds only at steady-state and for slow transients.

Frequency and active power control

Droop controllers use negative feedback to regulate the frequency, and to match the mechanical power to the instantaneous load. The main idea is demonstrated in Fig. 20. According to the swing equation in (59), when the electrical load increases the rotor frequency tends to decrease. The droop controller responds to this change in frequency and increases the mechanical power, such that at steady state the mechanical power and electrical power are equal.

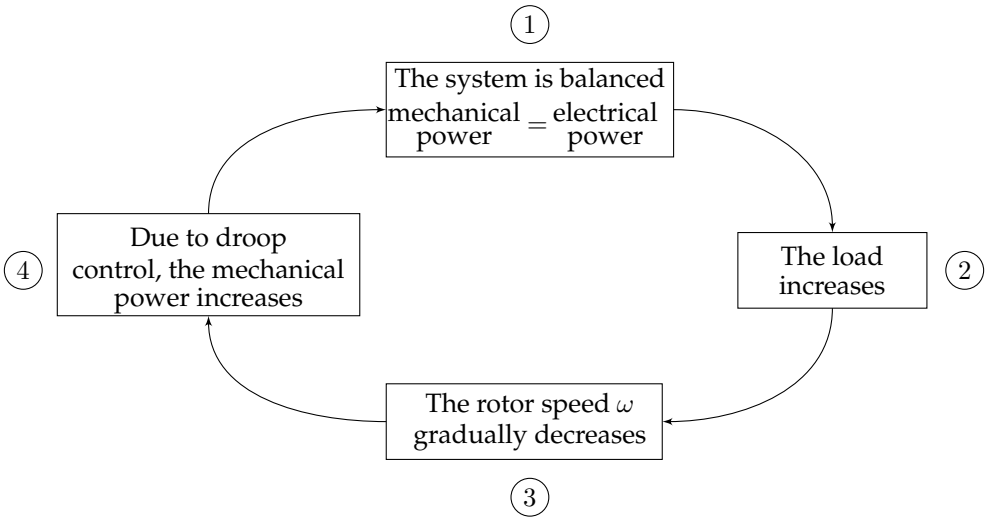

Figure 20: Conceptual operation of the droop control mechanism.

As an example, consider a generator connected to a single load, as shown in Fig. 21.

Figure 21: Example: generator connected to a single load.

A block diagram of this system is shown in Fig. 22.

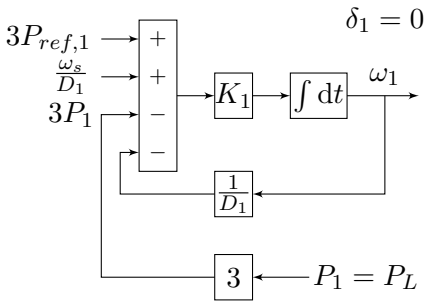

Figure 22: Generator connected to a single load: block diagram.

In order to stabilize the frequency, the mechanical power must be adjusted to match the instantaneous load. With no droop control ($D_1 = \infty$) we have

$$\omega_1(t) = \omega_1(0) + 3K_1 \int_0^t P_{ref,1}(\tau) - P_L(\tau)\mathrm{d}\tau. \tag{60}$$

Since in general $P_{ref,1}(t) \neq P_L(t)$ the frequency $\omega_1(t)$ does not converge to a finite value. In other words, with no droop control the system is unstable, since the mechanical power is not matched to the momentary load. Now, assuming that the droop control is active (D_1 is finite) we obtain

$$\frac{\mathrm{d}}{\mathrm{d}t}\omega_1 = \underbrace{-\frac{K_1}{D_1}}_{A}\omega_1 + \underbrace{K_1\left(3P_{ref,1} - 3P_L + \frac{\omega_s}{D_1}\right)}_{Bu}. \tag{61}$$

This dynamic system has a single pole on the left side of the complex plane, and is therefore stable. Typical waveforms are shown in Fig. 23.

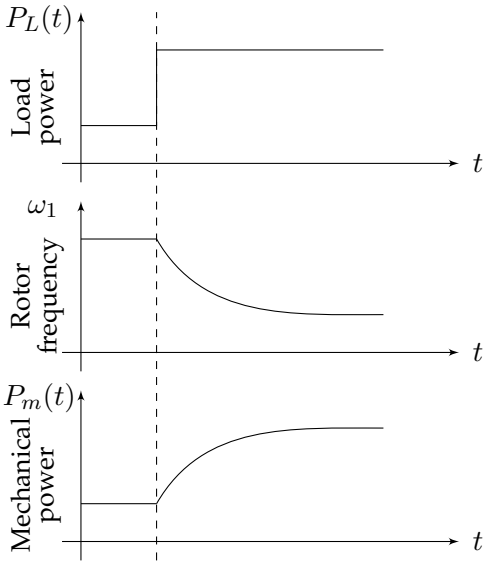

Figure 23: Generator connected to a single load: typical waveforms.

This example demonstrates how the droop control mechanism stabilizes the frequency of the system, by adjusting the mechanical power to match the electric load. The controller changes the mechanical power such that the frequency is stabilized, and at steady state the mechanical power and electrical power are equal.

Load sharing

Power systems often include many generators that operate in parallel. In an ideal system the total load is precisely known, and is shared among the generators according to their size and capacity. However in practice the load varies and cannot be predicted with absolute accuracy. Therefore, the instantaneous load should be shared in real time among the generators, while maintaining high efficiency and reliability. As we shall see in this section, this is one of the functions of the droop control mechanism.

To explain this idea we will now examine the equilibrium point of a multi-machine system, and show how it is affected by the droop control parameters. Consider a system with N generators, feeding a total load P_L. It is assumed that

- ✓ The system is not connected to an infinite bus.
- ✓ The generators and transmission network are lossless.

Recall that the swing equation is

$$\frac{\mathrm{d}}{\mathrm{d}t}\omega_i = K_i(P_{m,i} - 3P_i). \tag{62}$$

At equilibrium the time derivatives are zero, and therefore

$$\bar{P}_{m,i} = 3\bar{P}_i. \tag{63}$$

Substituting this expression in the droop equation yields

$$3\bar{P}_i = 3\bar{P}_{ref,i} - \frac{1}{D_i}(\bar{\omega}_i - \omega_s), \tag{64}$$

or equivalently

$$3D_i\bar{P}_i + (\bar{\omega}_i - \omega_s) = 3D_i\bar{P}_{ref,i}. \tag{65}$$

In addition

$$\frac{\mathrm{d}}{\mathrm{d}t}\delta_i = \omega_i - \omega_1. \tag{66}$$

At equilibrium the derivatives are equal to zero, so the frequencies must be equal:

$$\bar{\omega}_1 = \bar{\omega}_2 = \cdots = \bar{\omega}_N = \bar{\omega}. \tag{67}$$

Furthermore, since the network is assumed to be lossless we have

$$\sum_{i=1}^{N} \bar{P}_i = \bar{P}_L. \tag{68}$$

To summarize, the equilibrium point is characterized by the following equations:

$$\begin{aligned} 3D_i\bar{P}_i + (\bar{\omega} - \omega_s) &= 3D_i\bar{P}_{ref,i}, \\ \sum_{i=1}^{N} \bar{P}_i &= \bar{P}_L, \end{aligned} \tag{69}$$

or equivalently in matrix form:

$$\begin{bmatrix} 3D_1 & 0 & 0 & 1 \\ 0 & \ddots & 0 & \vdots \\ 0 & 0 & 3D_N & 1 \\ 1 & \cdots & 1 & 0 \end{bmatrix} \begin{bmatrix} \bar{P}_1 \\ \vdots \\ \bar{P}_N \\ \bar{\omega} - \omega_s \end{bmatrix}_{(N+1)\times 1} = \begin{bmatrix} 3D_1\bar{P}_{ref,1} \\ \vdots \\ 3D_N\bar{P}_{ref,N} \\ \bar{P}_L \end{bmatrix}_{(N+1)\times 1}, \tag{70}$$

which yields

$$\begin{aligned} \bar{\omega} &= \omega_s - 3\left(\sum_{i=1}^{N} \frac{1}{D_i}\right)^{-1} \left(\bar{P}_L - \sum_{i=1}^{N} \bar{P}_{ref,i}\right), \\ \bar{P}_i &= \bar{P}_{ref,i} - \frac{1}{3D_i}\left(\bar{\omega} - \omega_s\right). \end{aligned} \tag{71}$$

These are the frequencies and powers of the generators at equilibrium. For instance, for a system with two generators the equilibrium point is

$$\begin{aligned} \bar{\omega} &= \omega_s - \frac{3D_1D_2}{D_1 + D_2}\left(\bar{P}_L - \bar{P}_{ref,1} - \bar{P}_{ref,2}\right), \\ \bar{P}_1 &= \bar{P}_{ref,1} - \frac{1}{3D_1}\left(\bar{\omega} - \omega_s\right), \\ \bar{P}_2 &= \bar{P}_{ref,2} - \frac{1}{3D_2}\left(\bar{\omega} - \omega_s\right). \end{aligned} \tag{72}$$

Ideally, if the load is precisely known, the reference powers are selected such that their sum is equal to the total load:

$$\sum_{i=1}^{N} \bar{P}_{ref,i} = \bar{P}_L, \tag{73}$$

and accordingly,

$$\begin{aligned} \bar{\omega} &= \omega_s, \\ \bar{P}_i &= \bar{P}_{ref,i}. \end{aligned} \tag{74}$$

In other words, if the load power is precisely known then the frequency is equal to the nominal frequency, and the generators' powers are precisely equal to the reference powers. However, in practical systems the load varies, and cannot be predicted with absolute accuracy. Therefore, the difference between the actual load and the predicted load must be distributed among the generators. Based on (71) when the load exceeds its expected value:

- ✓ the frequency is smaller than the nominal frequency: $\bar{\omega} < \omega_s$.
- ✓ the powers are larger than the reference powers: $\bar{P}_i > \bar{P}_{ref,i}$.

When the load is lower than the expected value these inequalities are reversed.

The following discussion explains how the damping coefficients D_i affect the powers and frequency at steady-state. Consider first a system with two generators. According to (72),

- ✓ For $D_1 = D_2$ and $\bar{P}_{ref,1} = \bar{P}_{ref,2}$,

$$\bar{P}_1 = \bar{P}_2 = \frac{\bar{P}_L}{2}. \tag{75}$$

  In this case the power of the load is divided equally between the two generators.

- ✓ For a constant D_1 and $D_2 \to 0$,

$$\begin{aligned} \bar{\omega} &= \omega_s, \\ \bar{P}_1 &= \bar{P}_{ref,1}, \\ \bar{P}_2 &= \bar{P}_L - \bar{P}_{ref,1}. \end{aligned} \tag{76}$$

  In this case generator 1 provides constant power and generator 2 balances the power in the system and regulates the frequency. In other words, generator 1 is operated as a **power source**, while generator 2 is operated as an **infinite bus**.

More generally, the relationship between the active power and frequency at steady state are illustrated in Fig. 24.

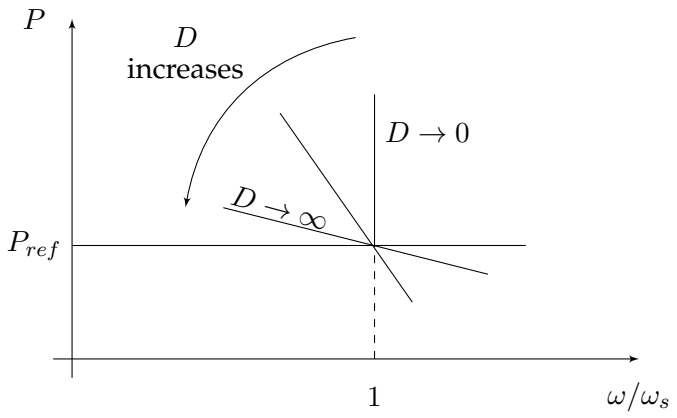

Figure 24: Droop characteristics in steady state: active power as a function of frequency.

The droop controller operates as follows:

- ✓ In case $D \to 0$:
  - The frequency ω is constant such that $\omega \approx \omega_s$. The generator provides active power as needed to stabilize the frequency.
  - The generator operates as an *infinite bus*.
- ✓ In case $D \to \infty$:
  - The active power is constant, $P \approx P_{ref}$.
  - The generator operates as a *power source*.
- ✓ Middle values of D:
  - The active power is regulated, but is not constant. The generator provides variable active power to adjust the frequency.
  - The frequency ω is regulated, but is not constant.

The analysis above explains the approximation of the *infinite bus*, which is used throughout this text. An infinite bus is a generator (or a group of generators) with a constant voltage amplitude that rotates at a constant frequency. In order to regulate the frequency, the infinite bus provides the power difference required to support the total load, and as a result maintains power balance within the grid.

Next we explain how the damping coefficients D_i are usually chosen.

- ✓ **Small generators** can provide limited power, and usually have high operation costs. Such generators should maintain relatively constant power and therefore use high values of D_i. When $D_i \to \infty$ the generator is operated as a *power source*.
- ✓ **Large generators** can provide more power, and usually have lower operation costs. Such generators use lower values of D_i in order to regulate the grid frequency. When $D_i \to 0$ the generator is operated as an *infinite bus*.

According to these guidelines, D_i is often chosen to be inversely proportional to the rated power of the generator:

$$D_i = \alpha \frac{\omega_s}{P_{rt,i}}, \tag{77}$$

where

- ✓ α is called the *droop percentage*. In typical systems, this constant is nearly equal for all generators.
- ✓ $P_{rt,i}$ is the rated power of the generator (the nominal three-phase power).

The following analysis explains the meaning of the droop percentage α. The droop equation (64) yields

$$\bar{\omega} = \omega_s + D_i \left(3\bar{P}_{ref,i} - 3\bar{P}_i\right). \tag{78}$$

Based on this equation the frequencies with no load and at full load are defined as follows:

$$\begin{aligned} \text{frequency at no load} &= \omega_{\text{no-load}} = \bar{\omega}|_{\bar{P}_i=0} = \omega_s + 3D_i\bar{P}_{ref,i}, \\ \text{frequency at full load} &= \omega_{\text{full-load}} = \bar{\omega}|_{\bar{P}_i=P_{rt,i}/3} = \omega_s + D_i\left(3\bar{P}_{ref,i} - P_{rt,i}\right), \end{aligned} \tag{79}$$

and α is given by

$$\alpha = \frac{D_i P_{rt,i}}{\omega_s} = \frac{\omega_{\text{no-load}} - \omega_{\text{full-load}}}{\omega_s}. \tag{80}$$

As a result α is the relative change in frequency when the generator operates with no load and at full load. A typical value is $\alpha \approx 5\%$.

When D_i are selected according to (77), the active power is distributed among the generators such that larger generators tend to provide more power. To see this, substitute $D_i = (\alpha\omega_s)/P_{rt,i}$ in the droop equation (64), and use (71) to obtain

$$\begin{aligned}
\bar{P}_i &= \bar{P}_{ref,i} - \frac{1}{3D_i}(\bar{\omega} - \omega_s) \\
&= \bar{P}_{ref,i} + \frac{1}{D_i}\left(\sum_{k=1}^{N}\frac{1}{D_k}\right)^{-1}\left(\bar{P}_L - \sum_{k=1}^{N}\bar{P}_{ref,k}\right) \\
&= \bar{P}_{ref,i} + \frac{P_{rt,i}}{\alpha\omega_s}\left(\sum_{k=1}^{N}\frac{P_{rt,k}}{\alpha\omega_s}\right)^{-1}\left(\bar{P}_L - \sum_{k=1}^{N}\bar{P}_{ref,k}\right) \\
&= \bar{P}_{ref,i} + P_{rt,i}\left(\sum_{k=1}^{N}P_{rt,k}\right)^{-1}\left(\bar{P}_L - \sum_{k=1}^{N}\bar{P}_{ref,k}\right), \\
&= \bar{P}_{ref,i} + \frac{P_{rt,i}}{P_{rt,tot}}\left(\bar{P}_L - \sum_{k=1}^{N}\bar{P}_{ref,k}\right),
\end{aligned} \tag{81}$$

where $P_{rt,tot} = \sum_{k=1}^{N} P_{rt,k}$. Based on this result deviations of the load from the reference power are divided between the generators, such that the change in power is **proportional to the rated power**. Therefore, the load is fairly distributed among the generators, according to their size and capacity.

Hierarchical control of power systems

Power grids are often operated by hierarchical control systems with (at least) two levels [29]:

- ✓ **Primary control**. This is the droop control mechanism we have discussed so far. This control loop is *fast*, implemented *locally* in each generator, and responds to instantaneous changes in the load power. Its main functions are to stabilize the frequency, and to promote fair sharing of active power among the generators.
- ✓ **Secondary control**. This is a *slow*, *centralized* control system that updates the reference powers to match the predicted load, such that $\sum_{i=1}^{N}\bar{P}_{ref,i} \approx \bar{P}_L$. This control level adjusts the active power production of the generators, and restores the frequency back to its nominal value following an imbalance.

The load power in a practical system is always varying, and cannot be predicted with absolute accuracy. The primary control system (droop control) responds to these changes, and regulates the active powers and frequency as discussed so far, according to (71). Over time, the load power deviates considerably from the reference power, and as a result there is a relatively large shift in frequency. This is resolved by the secondary control system that updates the reference powers such that $\sum_{i=1}^{N}\bar{P}_{ref,i} \approx \bar{P}_L$, which restores the frequency back to its nominal value. Typical waveforms are shown in Fig. 25, and the combined control system is illustrated in Fig. 26.

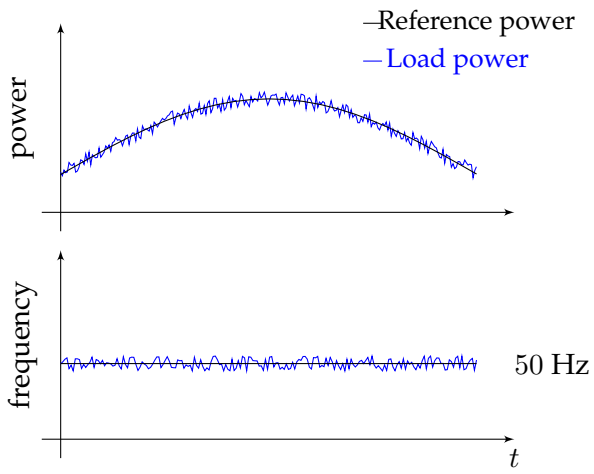

Figure 25: Random variations in power and frequency in a typical system.

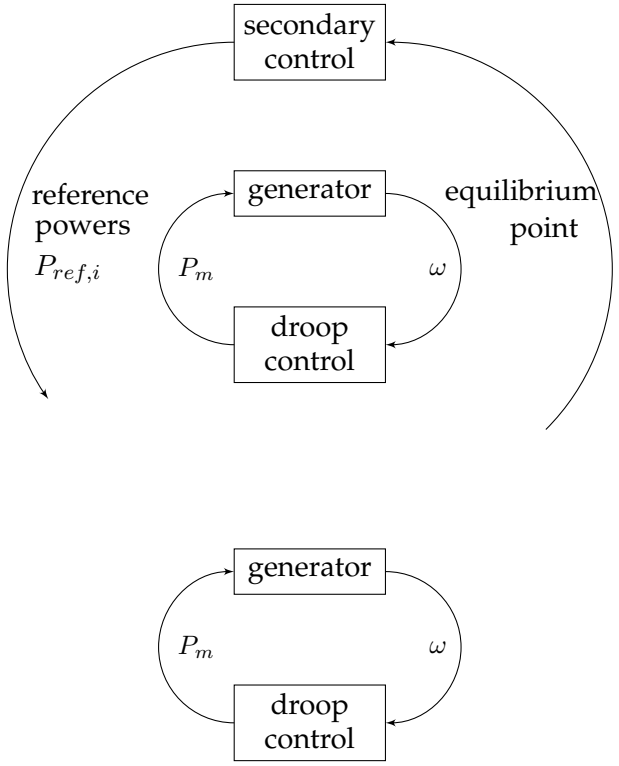

Secondary control:

- ✓ slow
- ✓ centralized
- ✓ restores frequency to nominal value following an imbalance
- ✓ adjusts active powers to operate the generators economically

Primary controllers:

- ✓ fast
- ✓ implemented locally
- ✓ regulate the frequency
- ✓ promote fair sharing of active power

Figure 26: Primary and Secondary control loops.

Several advantages of this control method are:

- ✓ The primary control loops are implemented locally in each generator, and share information only by means of the grid frequency.
- ✓ There is no need to transmit broad-band data between the generators.
- ✓ There is no central controller, and therefore no single point of failure.

✓ Generators can be added or removed from the system without changing the local controllers of other generators.

Due to these advantages the primary and secondary control loops form a distributed control system which is simple, efficient and reliable.

Voltage droop control

As discussed in the previous section the frequency droop mechanism controls the active power in order to regulate the frequency. Similarly, the voltage droop mechanism controls the generator's **voltage** in order to regulate the **reactive power**.

Consider a generator represented in steady state as a voltage source behind a series reactance, as described in Fig. 27. The reactive power Q may be found based on the circuit in

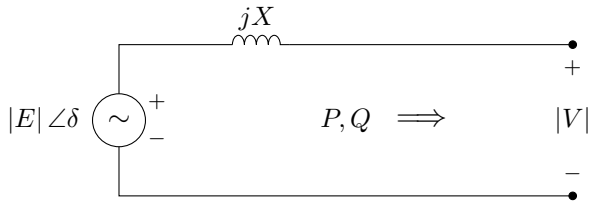

Figure 27: The generator is modeled in steady state as a voltage source behind a series reactance.

Fig. 27, and is given by

$$Q = \frac{|V|}{X}\left(|E|\cos(\delta) - |V|\right). \tag{82}$$

Assuming $\delta \to 0$ and $|E| \approx |V|$ this expression may be approximated as

$$\begin{aligned} Q &\approx \frac{|E|}{X}\left(|E| - |V|\right) \\ &\approx \frac{|E|^2}{X}\left(1 - \frac{|V|}{|E|}\right). \end{aligned} \tag{83}$$

The reactive power as a function of voltage is plotted in Fig. 28.

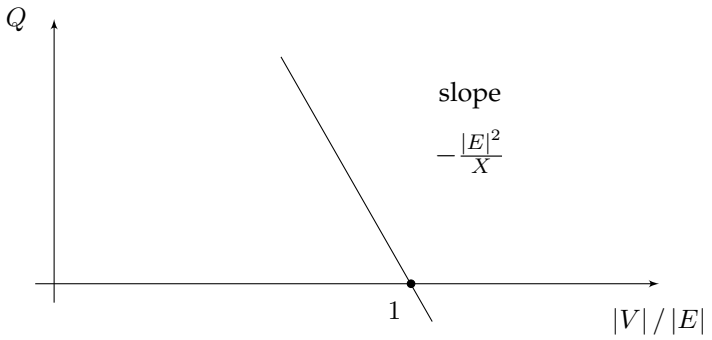

Figure 28: Reactive power as a function of voltage. Variations in $|V|$ may result in high and unpredictable reactive power flow.

If the voltage $|E|$ is fixed then variations in $|V|$ may result in high and unpredictable reactive power flow. This is potentially dangerous since high reactive power causes losses, and may lead to reliability issues. To solve this problem the voltage droop mechanism regulates the reactive power by adjusting $|E|$ in inverse proportion to Q:

$$|E| = E_{ref} - k_q(Q - Q_{ref}), \tag{84}$$

where

- ✓ E_{ref} is the reference voltage
- ✓ Q_{ref} is the reference reactive power
- ✓ k_q is a constant

In a synchronous generator this control law is implemented in practice by adjusting the current in the field winding. Note that (84) is an approximated expression which only holds for slow transients.
Substitution of (84) in (83) yields

$$Q \approx \frac{|E|}{X}\left(|E| - |V|\right) \approx \frac{E_{ref}}{X}\left(E_{ref} - k_q(Q - Q_{ref}) - |V|\right), \tag{85}$$

which following several algebraic manipulations may be written as

$$Q = \frac{E_{ref}}{X + E_{ref}k_q}\left(E_{ref} + k_q Q_{ref} - |V|\right). \tag{86}$$

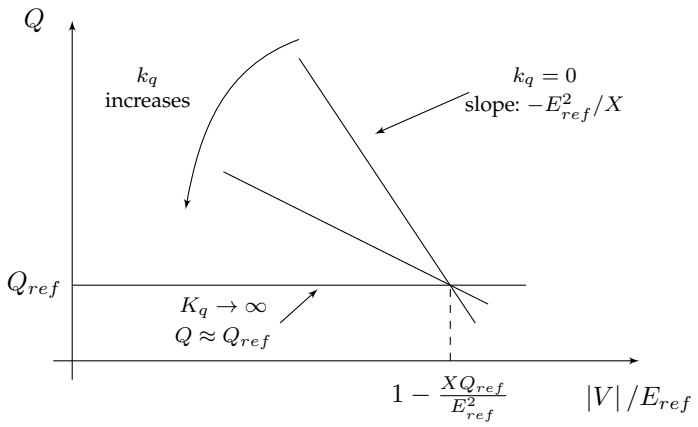

Figure 29: Droop characteristics in steady state: reactive power as a function of voltage.

In steady state the controller operates as follows:

In case $k_q = 0$ (no voltage droop):

- ✓ The reactive power is not regulated.
- ✓ If X is small then $|V| \approx E_{ref}$, and the generator operates as a voltage source.

In case $k_q \to \infty$:

- ✓ The reactive power is constant: $Q \approx Q_{ref}$.
- ✓ The voltage $|V|$ is not regulated.

Middle values of k_q:

- ✓ Combine the properties of these two extreme cases.
- ✓ The reactive power and voltage are regulated, but are not constant.

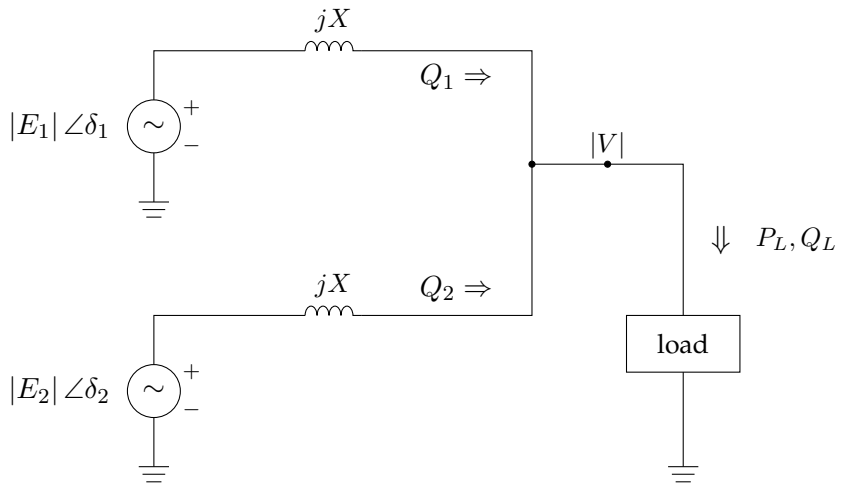

Figure 30: Example: reactive power sharing between two generators.

An additional objective of the voltage droop mechanism is to properly share reactive power among the generators. As an example consider the system in Fig. 30. In steady-state this system is described by the following set of equations:

$$\begin{aligned} Q_1 &\approx \frac{|E_1|}{X}\left(|E_1| - |V|\right), \\ Q_2 &\approx \frac{|E_2|}{X}\left(|E_2| - |V|\right), \\ |E_1| &= E_{ref,1} - k_{q,1}(Q_1 - Q_{ref,1}), \\ |E_2| &= E_{ref,2} - k_{q,2}(Q_2 - Q_{ref,2}), \\ Q_L &= Q_1 + Q_2. \end{aligned} \tag{87}$$

Assume first that there is no droop control ($k_{q,1} = k_{q,2} = 0$), and $Q_L = 0$. The resulting reactive powers in this case are

$$Q_1 = -Q_2 = \frac{|E_1||E_2|}{X}\frac{|E_1| - |E_2|}{|E_1| + |E_2|}. \tag{88}$$

Here, even though $Q_L = 0$, there may be significant reactive power flow between the two generators. Now assume that the droop controller is active, and

$$\begin{aligned} k_{q,1} &= k_{q,2} = k_q, \\ E_{ref,1} &= E_{ref,2} = E_{ref}, \\ Q_{ref,1} &= Q_{ref,2} = Q_{ref}. \end{aligned} \tag{89}$$

The resulting reactive powers in this case are

$$Q_1 = Q_2 = \frac{Q_L}{2}. \tag{90}$$

The controller shares the reactive power evenly between the two generators, and therefore prevents circulation of reactive power.

Example

This example demonstrates the analysis of a typical time-varying phasor model. Consider two synchronous machines feeding a resistive load, as illustrated in Fig. 31.

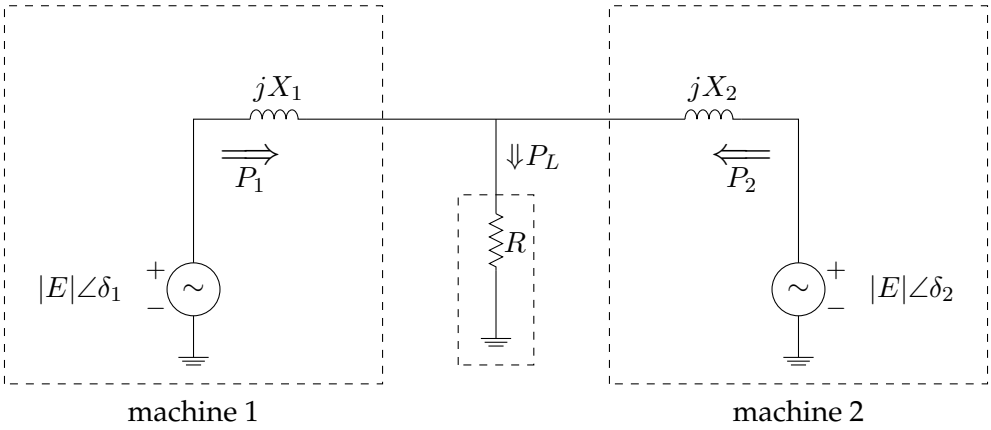

Figure 31: Example: two synchronous machines feeding a resistive load, single-phase diagram.

In this example there is no infinite bus, so phasors are referenced to the rotor angle of the first machine, that is $\theta_r = \theta_1 + \frac{\pi}{2}$. This choice yields

$$\begin{aligned} \delta_1 &= \theta_1 - \left(\theta_1 + \frac{\pi}{2}\right) + \frac{\pi}{2} = 0, \\ \delta_2 &= \theta_2 - \left(\theta_1 + \frac{\pi}{2}\right) + \frac{\pi}{2} = \theta_2 - \theta_1, \\ \frac{\mathrm{d}}{\mathrm{d}t}\delta_2 &= \omega_2 - \omega_1. \end{aligned} \tag{91}$$

A block diagram of the resulting system is shown in Fig. 32.

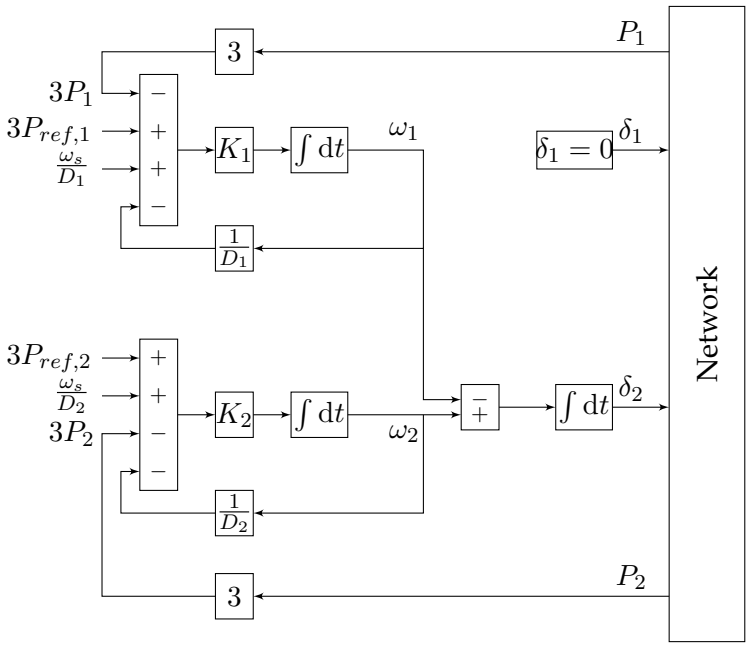

Figure 32: Two machines example: block diagram.

The network and load are described using the DC power flow approximation. To this end:

- ✓ Assume that the voltages across the network are equal to $|E|$.
- ✓ The active power flowing into the load is $P_L = |E|^2/R$.

Based on these assumptions, the network equations are

$$\begin{aligned} \delta_1 &= 0, \\ P_1 &= \frac{|E|^2}{X_1}\left(\delta_1 - \delta_3\right), \\ P_2 &= \frac{|E|^2}{X_2}\left(\delta_2 - \delta_3\right), \\ P_1 + P_2 &= P_L, \end{aligned} \tag{92}$$

where δ_3 is the voltage phase on the load resistor R. These equations lead to

$$\begin{aligned} P_1 &= \frac{X_2}{X_1+X_2}P_L - \frac{|E|^2}{X_1+X_2}\delta_2, \\ P_2 &= \frac{X_1}{X_1+X_2}P_L + \frac{|E|^2}{X_1+X_2}\delta_2. \end{aligned} \tag{93}$$

The state variables are chosen as the outputs of the three integrators, that is

$$x = \begin{bmatrix} x_1 \\ x_2 \\ x_3 \end{bmatrix} = \begin{bmatrix} \delta_2 \\ \omega_1 \\ \omega_2 \end{bmatrix}. \tag{94}$$

In addition, the inputs are

$$u = \begin{bmatrix} P_{ref,1} \\ P_{ref,2} \end{bmatrix}, \tag{95}$$

and the system outputs are (arbitrarily) chosen as

$$y = \begin{bmatrix} \omega_1 \\ \omega_2 \end{bmatrix}. \tag{96}$$

The resulting state-space model is

$$\begin{aligned} \frac{\mathrm{d}}{\mathrm{d}t}\begin{bmatrix} \delta_2 \\ \omega_1 \\ \omega_2 \end{bmatrix} &= \begin{bmatrix} 0 & -1 & +1 \\ \frac{3K_1|E|^2}{X_1+X_2} & -\frac{K_1}{D_1} & 0 \\ -\frac{3K_2|E|^2}{X_1+X_2} & 0 & -\frac{K_2}{D_2} \end{bmatrix}\begin{bmatrix} \delta_2 \\ \omega_1 \\ \omega_2 \end{bmatrix} + \begin{bmatrix} 0 & 0 \\ 3K_1 & 0 \\ 0 & 3K_2 \end{bmatrix}\begin{bmatrix} P_{ref,1} \\ P_{ref,2} \end{bmatrix} + \begin{bmatrix} 0 \\ C_1 \\ C_2 \end{bmatrix}, \\ \begin{bmatrix} \omega_1 \\ \omega_2 \end{bmatrix} &= \begin{bmatrix} 0 & 1 & 0 \\ 0 & 0 & 1 \end{bmatrix}\begin{bmatrix} \delta_2 \\ \omega_1 \\ \omega_2 \end{bmatrix}, \end{aligned} \tag{97}$$

where $C_1 = \frac{K_1\omega_s}{D_1} - \frac{3K_1X_2P_L}{X_1+X_2}$ and $C_2 = \frac{K_2\omega_s}{D_2} - \frac{3K_2X_1P_L}{X_1+X_2}$. Note that this model is linear, as a result of using the DC power flow approximation.

The model above is not yet in standard form, due to the vector of constants on the right. To obtain a standard linear model define the small-signals

$$\begin{aligned} \hat{\delta}_2 &= \delta_2 - \bar{\delta}_2, \\ \hat{\omega}_1 &= \omega_1 - \bar{\omega}_1, \\ \hat{\omega}_2 &= \omega_2 - \bar{\omega}_2, \end{aligned} \tag{98}$$

where $\bar{\delta}_2, \bar{\omega}_1, \bar{\omega}_2$ denote the equilibrium point. The resulting linearized system is

$$\begin{aligned}\frac{\mathrm{d}}{\mathrm{d}t}\begin{bmatrix}\hat{\delta}_2\\ \hat{\omega}_1\\ \hat{\omega}_2\end{bmatrix} &= \begin{bmatrix}0 & -1 & 1\\ \frac{3K_1|E|^2}{X_1+X_2} & -\frac{K_1}{D_1} & 0\\ -\frac{3K_2|E|^2}{X_1+X_2} & 0 & -\frac{K_2}{D_2}\end{bmatrix}\begin{bmatrix}\hat{\delta}_2\\ \hat{\omega}_1\\ \hat{\omega}_2\end{bmatrix} + \begin{bmatrix}0 & 0\\ 3K_1 & 0\\ 0 & 3K_2\end{bmatrix}\begin{bmatrix}\hat{P}_{ref,1}\\ \hat{P}_{ref,2}\end{bmatrix},\\ \begin{bmatrix}\hat{\omega}_1\\ \hat{\omega}_2\end{bmatrix} &= \begin{bmatrix}0 & 1 & 0\\ 0 & 0 & 1\end{bmatrix}\begin{bmatrix}\hat{\delta}_2\\ \hat{\omega}_1\\ \hat{\omega}_2\end{bmatrix}.\end{aligned} \tag{99}$$

This model is identical to the model in (97), except that the vector of constants has been eliminated. The same model can also be obtained by linearizing the block diagram directly. This is done by

- ✓ Replacing all signals with "small" signals;
- ✓ Zeroing all the constants;
- ✓ Replacing memoryless nonlinear functions by constant gains, which are the functions' derivatives at the equilibrium point.

The model in (99) can now be analyzed based on standard linear systems theory.

References

[1] P. Kundur, J. Paserba, V. Ajjarapu, G. Andersson, A. Bose, C. Canizares, N. Hatziargyriou, D. Hill, A. Stankovic, C. Taylor, T. Van Cutsem, and V. Vittal, "Definition and classification of power system stability IEEE/CIGRE joint task force on stability terms and definitions," *IEEE Trans. Power Syst.*, vol. 19, pp. 1387–1401, 2004.

[2] J. Machowski, J. Bialek, and J. Bumby, *Power Dystem Dynamics: Stability and Control*. John Wiley & Sons, 2011.

[3] T. Van Cutsem and C. Vournas, *Voltage Stability of Electric Power Systems*. Norwell, MA: Kluwer Academic Publishers, 1998.

[4] A. J. Wood, B. F. Wollenberg, and G. B. Sheble, *Power Generation, Operation, and Control*. John Wiley & Sons, 2013.

[5] P. M. Anderson and A. A. Fouad, *Power System Control and Stability*. John Wiley & Sons, 2008.

[6] J. J. Grainger and W. D. Stevenson, *Power System Analysis*. New York: McGraw-Hill, 1994.

[7] M. Ilić and J. Zaborszky, *Dynamics and Control of Large Electric Power Systems*. New York: Wiley, 2000.

[8] P. Kundur, *Power system stability and control*. McGraw-Hill, 1994.

[9] Y. Liu, K. Sun, and Y. Liu, "A measurement-based power system model for dynamic response estimation and instability warning," *Electr. Power Syst. Res.*, vol. 124, pp. 1–9, 2015.

[10] L. Miller, L. Cibulka, M. Brown, and A. von Meier, "Electric distribution system models for renewable integration: Status and research gaps analysis," California Energy Commission, CA, USA, Tech. Rep. CEC-500-10-055, 2013.

[11] H. Saadat, *Power System Analysis*. PSA Publishing, 2010.

[12] W. D. Stevenson, *Elements of Power System Analysis*, 4th ed., ser. Electrical and Electronic Engineering Series, F. E. Terman, Ed. New York: McGraw-Hill, 1982.

[13] R. Teodorescu, M. Liserre, and P. Rodriguez, *Grid Converters for Photovoltaic and Wind Power Systems*. John Wiley & Sons, 2011.

[14] R. Yousefian and S. Kamalasadan, "A Lyapunov function based optimal hybrid power system controller for improved transient stability," *Electr. Power Syst. Res.*, vol. 137, pp. 6–15, 2016.

[15] P. C. Krause, O. Wasynczuk, S. D. Sudhoff, and S. Pekarek, *Analysis of Electric Machinery and Drive Systems*, 3rd ed. Wiley-IEEE Press, 2013.

[16] M. A. Pai, P. W. Sauer, and B. C. Lesieutre, "Static and dynamic nonlinear loads and structural stability in power systems," *Proc. IEEE*, vol. 83, no. 11, pp. 1562–1572, 1995.

[17] P. W. Sauer and M. A. Pai, *Power system dynamics and stability*. Upper Saddle River, New Jersey: Prentice Hall, 1998.

[18] T. Wildi, *Electrical Machines, Drives and Power Systems*, 5th ed. Upper Saddle River, NJ, USA: Pearson Education, 2002.

[19] T. H. Demiray, "Simulation of power system dynamics using dynamic phasor models," Ph.D. dissertation, 2008.

[20] M. Ilić, R. Jaddivada, and X. Miao, "Modeling and analysis methods for assessing stability of microgrids," *IFAC-PapersOnLine*, vol. 50, no. 1, pp. 5448–5455, 2017.

[21] J. Belikov and Y. Levron, "A sparse minimal-order dynamic model of power networks based on dq0 signals," *IEEE Trans. Power Syst.*, vol. 33, no. 1, pp. 1059–1067, 2018.

[22] J. Belikov and Y. Levron, "Comparison of time-varying phasor and dq0 dynamic models for large transmission networks," *Int. J. Elec. Power*, vol. 93, pp. 65–74, 2017.

[23] D. Baimel, J. Belikov, J. M. Guerrero, and Y. Levron, "Dynamic modeling of networks, microgrids, and renewable sources in the dq0 reference frame: A survey," *IEEE Access*, vol. 5, pp. 21 323–21 335, 2017.

[24] J. Schiffer, D. Zonetti, R. Ortega, A. M. Stanković, T. Sezi, and J. Raisch, "A survey on modeling of microgrids—From fundamental physics to phasors and voltage sources," *Automatica*, vol. 74, pp. 135–150, 2016.

[25] A. M. Stanković, S. R. Sanders, and T. Aydin, "Dynamic phasors in modeling and analysis of unbalanced polyphase AC machines," *IEEE Trans. Energy Convers.*, vol. 17, no. 1, pp. 107–113, 2002.

[26] F. Milano, F. Dörfler, G. Hug, D. J. Hill, and G. Verbič, "Foundations and challenges of low-inertia systems," in *Power Systems Computation Conference*, 2018, pp. 1–25.

[27] T. Demiray, G. Andersson, and L. Busarello, "Evaluation study for the simulation of power system transients using dynamic phasor models," in *Transmission and Distribution Conference and Exposition*, 2008, pp. 1–6.

[28] A. E. Fitzgerald, C. Kingsley, and S. D. Umans, *Electric Machinery*, 6th ed. New York: McGraw-Hill, 2003.

[29] Y. G. Rebours, D. S. Kirschen, M. Trotignon, and S. Rossignol, "A survey of frequency and voltage control ancillary services—Part I: Technical features," *IEEE Trans. Power Syst.*, vol. 22, no. 1, pp. 350–357, 2007.